GCAGS JOURNAL
A Publication of the Gulf Coast Association of Geological Societies
www.gcags.org

The Effect of Sample Volume on Micro-Rebound Hammer UCS Measurements in Gulf Coast Cretaceous Carbonate Cores

Donnie Brooks, Xavier Janson, and Chris Zahm

Bureau of Economic Geology, Jackson School of Geosciences, University of Texas at Austin, University Station, Box X, Austin, Texas 78713–8924, U.S.A.

ABSTRACT

Micro-rebound hammers (MRHs) are nondestructive tools that are increasingly being used in mechanical characterization of core in reservoir characterization studies. The micro-rebound hammer responds to rock hardness as a proxy for unconfined compressive strength (UCS) but is sensitive to sample volume, rock heterogeneities, grain size, and macropore size. In this study, we systematically investigate the effect of sample volume on several rock types from both quarry and Cretaceous outcrops, using two different techniques for data collection. Our results show that a significant drop in MRH–derived UCS is observed below 12 in^3 (197 cm^3) of sample volume. This is relevant to most core-based study because the core material, typically preserved as a thinner archive side and a thicker sample side, is often fractured or broken into fragments of varying size. In addition, larger scatter in MRH–derived UCS values is observed for samples with heterogeneities such as bioturbation or large moldic pores, as well as samples with large grains. This study also shows that sample-volume effect seems not to greatly affect the relative values of MRH–derived UCS; therefore, the shape and trend of MRH–derived UCS curves on core are a reliable dataset that can be used for mechanical characterization in reservoir studies.

INTRODUCTION

Reservoir characterization projects often rely on a very limited amount of core-based information, with the bulk of the data coming from well logs. In carbonate rocks, making a reliable connection between the petrophysical properties of the reservoir rocks and the well log–derived static and elastic properties can be difficult, especially at the scale needed for most enhanced recovery projects. Moreover, understanding and characterizing the fundamental link between carbonate lithofacies, diagenesis, petrophysical properties, and unconfined compressive strength (UCS) is essential for predicting fracture susceptibility, both natural and stimulated.

Core data are paramount for establishing a relationship between UCS and other petrophysical characteristics. To capture most of the reservoir-scale heterogeneities, the number of data points collected needs to be high enough to establish a statistically valid relationship between measured UCS and other mechanical parameters, and to discern small-scale UCS contrasts. However, extensive plugging and testing of core plugs is very time consuming and expensive; in addition, adequate core material is not always available for a large number of core plugs.

Nondestructive methods are an attractive way to fill the gap between sparse 1 in (2.5 cm) diameter core-plug data (Viles et al., 2010; Zahm and Enderlin, 2010; Daniels et al., 2012). The data collected using a micro-rebound hammer (MRH) has been shown by various studies to be an acceptable approximation of UCS (Verwaal and Mulder, 1993; Aoki and Matsukura, 2008). The advantage of using a micro-rebound hammer is the ability to collect a large number of data points in a nondestructive manner in between strategically spaced plugs. A few documented pitfalls of using MRHs, however, include operator bias, mineralogy, sample size, sample preparation, sample anisotropy and heterogeneities, and grain sizes. MRHs have been shown quite early in their use to be sensitive to sample size (or volume) (Verwaal and Mulder, 1993). Because most reservoir-characterization projects will use MRHs on core with either a thick sample half or a thinner archive part, we attempted to systematically examine and quantify the sample-volume effect on several rock-mechanics standard blocks and various Cretaceous rock from Texas. The results were then compared to standard laboratory UCS measurements on 1 in plugs for each rock sample.

INSTRUMENTS AND METHODS

The Proceq Equotip MRH measures the initial and rebound velocities of a spring-loaded impact body (Asef, 1995). As it

Manuscript received March 25, 2016; revised manuscript received June 22, 2016; manuscript accepted July 8, 2016.

GCAGS Journal, v. 5 (2016), p. 189–202.

moves through a coil, a magnet in the metal impact body induces a current in the coil with a voltage proportional to its velocity. The ratio of rebound velocity to initial velocity is a measure of the sample's hardness (Asef, 1995). Sample hardness is used as a proxy for UCS as qualitatively demonstrated in several studies (Verwaal and Mulder, 1993; Aoki and Matsukura, 2008; Lee et al., 2014). The Equotip hardness measured in HLD units can be converted to UCS (MPa) using the following empirical relationship established by Zahm and Enderlin (2010):

$$\text{UCS (MPa)} = 0.000000683 * \text{HLD}^{2.9}. \qquad \text{(Eq. 1)}$$

In this relationship, sample volume is not considered as part of the correlation between measured HLD and UCS.

To perform standard UCS measurements (ASTM DD7012–13) on the 1 in core plugs, we used an RTR–1000, a standard commercial triaxial system from GCTS. The system consists of a load frame, a hydraulic pump unit, a controller unit, and sensors for measuring applied force and sample deformation. The load frame has a 1000 kN axial load capacity and a 1750 kN/mm frame stiffness. The triaxial cell can be pressurized up to a 140 MPa confining pressure. Axial and circumferential (radial) deformations of rock specimens are measured using miniature linear variable differential transformers (LVDT) mounted directly on the specimen. The test consists of gradually increasing the axial strain on the specimen at a rate of 0.045%/min until failure. Failure was inferred when deviator stress decreased abruptly by more than 5 MPa. Deviator stress at failure represents the UCS value for that sample.

We used six rock samples from quarries and six outcrop samples. For the quarried samples, we initially measured hardness on an 8 in x 8 in x 4 in (20 cm x 20 cm x 10 cm) block. Then we cut off a 2 in x 8 in x 4 in (5 cm x 20 cm x 10 cm) slice and repeated the measurements on the remaining 6 in x 8 in x 4 in block (15 cm x 20 cm x 10 cm). We repeated this process for 4 in x 8 in x 4 in (10 cm x 20 cm x 10 cm), 2 in x 8 in x 4 in (5 cm x 20 cm x 10 cm), and 1 in x 8 in x 4 in (2.5 cm x 20 cm x 10 cm) blocks (Fig. 1). For the outcrop hand samples, we started with the largest squarish block available and then reduced the volume incrementally. Additionally, we extracted 2 in (5 cm) diameter plugs from the quarried samples and 1 in (2.5 cm) diameter plugs from all samples and performed the same hardness measurements on the plugs as on the blocks.

Equotip measurements were collected using two different techniques reflective of the methods used in previous studies (Verwaal and Mulder, 1993; Aoki and Matsukura, 2008; Zahm and Enderlin, 2010). With the Separate Impacts Method, a single impact is applied at 10–20 separate points on the sample; the high and low HLD values are discarded, and the remaining values are averaged. With the Combined Impacts Method, 10 impacts are applied in the same spot; the high and low values are discarded, and the remaining values are averaged.

ROCK DESCRIPTIONS

We used the following quarried rock samples, which are rocks commonly used in rock-mechanics studies: Berea Sandstone, Indiana Limestone, Silurian Dolomite, Winterset Limestone, and Carthage Marble (see Table 1 and Figure 2). In addition, we used five samples (Fig. 2) from the Upper Glen Rose Formation that outcrops along Highway 360 in Austin, Texas (Phelps et al., 2013). This roadcut exposes excellent examples of Albian shelf-interior subtidal and peritidal cycles. We also used one sample from the Boquillas Formation (Fig. 2) collected on the roadcut outcrop of Highway 90 approximately 20 mi (32 km) northwest of Del Rio, Texas.

RESULTS

Plots of micro-rebound hammer–derived UCS (MRH–UCS) as a function of sample volume are shown in Figures 3 and 4. The error bars shown in Figure 4 were calculated from the standard deviations of the measurements and propagated through Equation 1 (Zahm and Enderlin, 2010). The data show that, although there was significant scatter for some samples, the results for the 1 in (2.5 cm) plug were consistently statistically the smallest. For all samples, the Separate method produced more consistent results, whereas using the Combined method led to both higher MRH–UCS values and much larger scatter in the data.

For the Berea Sandstone sample, the Separate method produced consistent results for samples larger than 2 in^3 (33 cm^3), which will hereafter be refered to as the large samples. The MRH–UCS value on the 1 in (2.5 cm) plug (2 in^3 [33cm^3]) is very close to the average of the large samples (Table 2). The Combined method shows a very similar trend, although with a large scatter and large shift toward higher MRH–UCS.

The first Indiana Limestone sample yielded an MRH–UCS value for the 1 in (2.5 cm) plug that is somewhat close to the average value for the large samples. The second Indiana Limestone sample is even closer, although there is a slightly larger scatter in the larger samples' values, with some MRH–UCS values in the large blocks very close to or slightly lower than the MRH–UCS of the 1 in (2.5 cm) plug. We see a consistent pattern of reduced MRH–UCS at the 1 in (2.5 cm) plug scale compared to the larger volumes in the Silurian Dolomite sample. The difference is significant: 41% for the Separate method and 27% for the Combined method.

For the Winterset Limestone, the Separate method led to a constantly decreasing MRH–UCS value from the largest volume to the 1 in (2.5 cm) plug. The Combined method resulted in the lowest value in the 125 in^3 (2050 cm^3) volume and higher-than-average values in the smaller volumes. Fortuitously, the largest-volume MRH–UCS value is almost identical to the 1 in (2.5 cm) plug value. No clear trend can be identified in the Carthage marble MRH–UCS value for the Separate method, with the MRH–UCS values varying above and below the large-sample average. For the Combined method, the 1 in (2.5 cm) plug MRH–UCS value is clearly lower than the average (18%).

In contrast to the rock-mechanics standard-quarry samples, the outcrop samples from the Glen Rose Formation generally show a more consistent pattern and less scatter.

The skeletal grainstone (S5) shows very consistent MRH–UCS values for the large samples and a 39% decrease at the 1 in (2.5 cm) plug for the Separate method. The Combined method led to slightly more scattered values, with no clear trend or even a slightly reverse trend (e.g., lower MRH–UCS values at the largest volume). The bioturbated wackestone (S16) displays a wider scatter in data, especially for the Combined method. The MRH–UCS values obtained with the Separate method show a similar 34% decrease at the 1 in (2.5 cm) plug scale compared to the average of the larger samples. The MRH–UCS values obtained with the Combined method show a negative correlation, with sample volume associated with a large scatter. Dolomitic mudstone (S19) and bioturbated dolomitic wackestone (S20) both have results very similar to S5: a clear pattern of decrease in MRH–UCS at the 1 in (2.5 cm) plug scale for the Separate method, and more scattered results for the Combined method although with a still-significant decrease of MRH–UCS at the 1 in (2.5 cm) plug scale.

The moldic skeletal dolopackstone (S22) shows very consistently low values of MRH–UCS for the Separate method, with a 40% decrease of the MRH–UCS at the 1 in (2.5 cm) plug scale. The Combined method shows a larger scatter and a significant drop (56%) of MRH–UCS at the 1 in (2.5 cm) plug scale. The cemented calcareous mudstone of the Boquillas Formation has the largest measured MRH–UCS of all the samples. The Sepa-

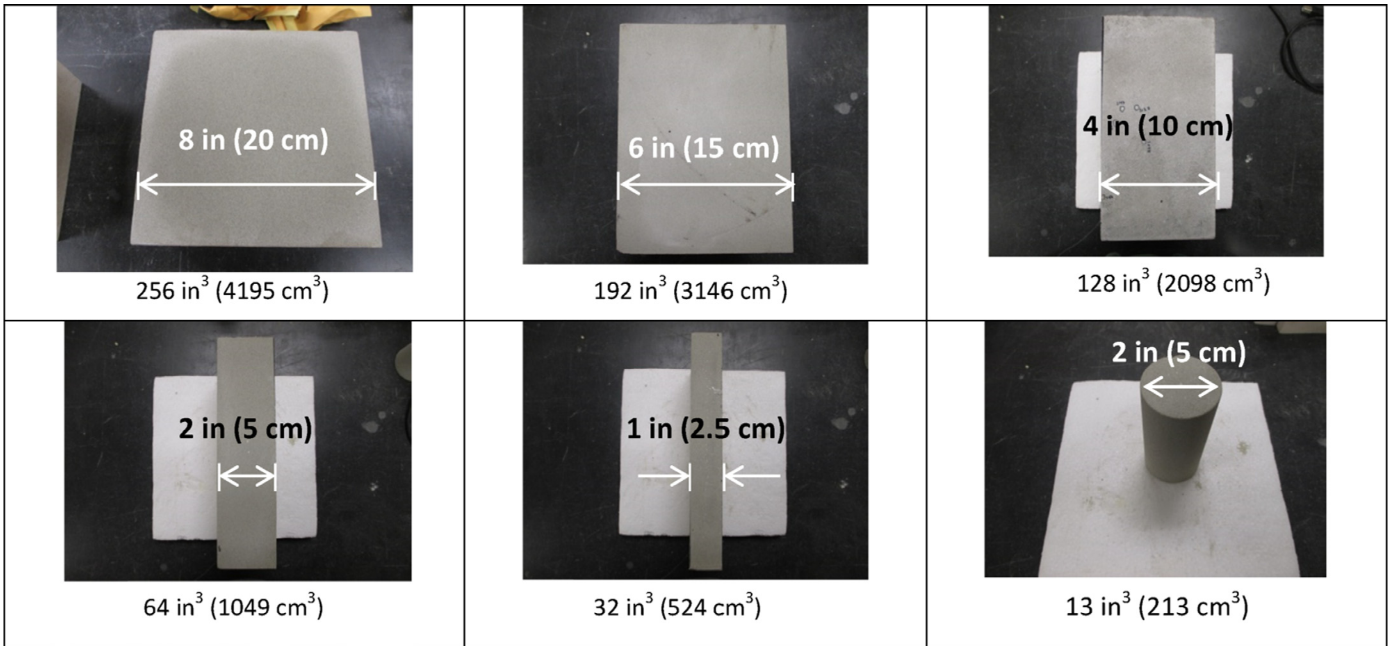

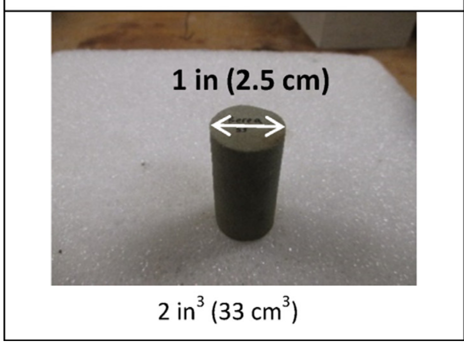

Figure 1. Sample sizes for quarried rock samples. MRH–UCS measurements were made on the 8 in (20 cm) block; the block was sawn to 6 in (15 cm) and the measurements repeated. The process was repeated down to the 1 in (2.5 cm) blocks. Plugs of 1 in (2.5 cm) and 2 in (5 cm) in diameter were drilled, and MRH–UCS measurements were made on each.

Table 1. Rock descriptions. The first five samples are from quarries; the Upper and Lower Cretaceous samples are from roadside outcrops in Texas.

Sample	Age	Description
Berea Sandstone	Mississippian	Well-sorted fine-grained sandstone
Indiana Limestone	Mississippian	Skeletal (bryozoan and crinoids) medium-sorted coarse-grained grainstone
Silurian Dolomite	Silurian	Coarse crystalline dolopackstone with vuggy porosity
Winterset Limestone	Upper Pennsylvanian	Skeletal and ooid grainstone with oomoldic porosity
Carthage Marble	Ordovician	Poorly sorted crinoidal rudstone
Boquillas Fm.	Upper Cretaceous (Turonian)	Calcareous mudstone
Glen Rose Fm. S5	Lower Cretaceous (Albian)	Skeletal (miliolids) grainstone
Glen Rose Fm. S16	Lower Cretaceous (Albian)	Bioturbated skeletal wackestone
Glen Rose Fm. S19	Lower Cretaceous (Albian)	Dolomudstone
Glen Rose Fm. S20	Lower Cretaceous (Albian)	Bioturbated dolowackestone
Glen Rose Fm. S22	Lower Cretaceous (Albian)	Skeletal moldic dolopackstone

rate method led to a 26% drop of MRH–UCS value at the 1 in (2.5 cm) plug scale compared to the larger volumes. MRH–UCS values for the larger volumes consistently decrease as volume decreases. MRH–UCS values for the Combined method are more scattered, with a significant drop of MRH–UCS occurring for a larger volume (24 in^3 [393 cm^3]).

Table 3 compiles the percent difference between UCS values obtained with the MRH and the ones measured on the 1 in (2.5 cm) sample in a triaxial device, using the standard ASTM procedure for determining UCS with a test to failure. It is apparent that the MRH–UCS on a 1 in (2.5 cm) plug is not the best approximation for the standard UCS measurement and will significantly differ from the UCS value. Figure 5 shows a cross plot of UCS measured in the laboratory and MRH–derived UCS for both methods: for the average of the large samples (Fig. 5A) and for the 1 in (2.5 cm) plugs (Fig. 5B). For the large samples, the Separate method values are closer to the "1:1" line, which is where the value would fall if MRH methods corresponded exactly to the

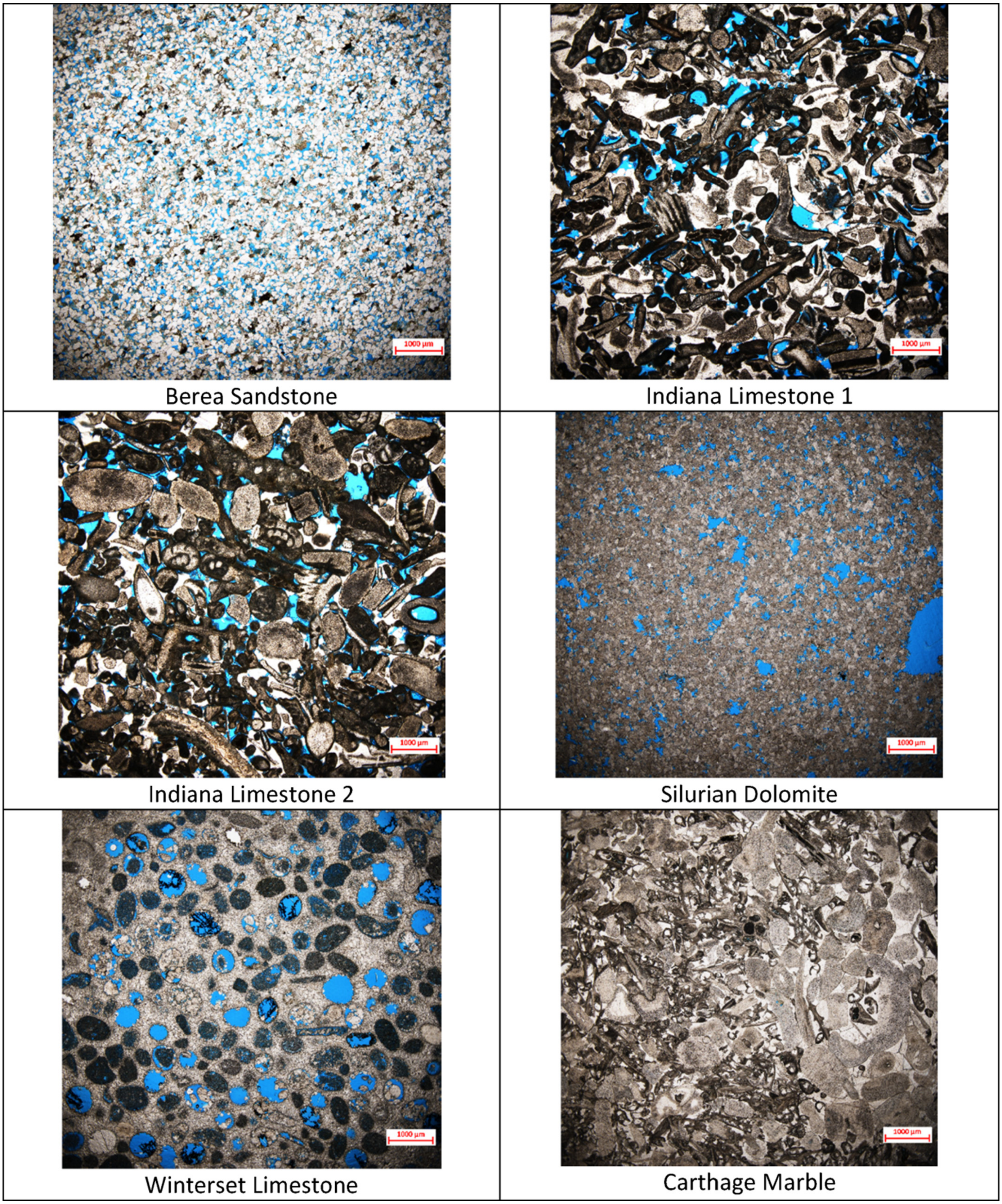

Figure 2. Thin-section photomicrographs of all samples. Blue color highlights pore space. Scale bar is 1000 µm for quarried rocks and 500 µm for outcrop samples. Figure continues on following page.

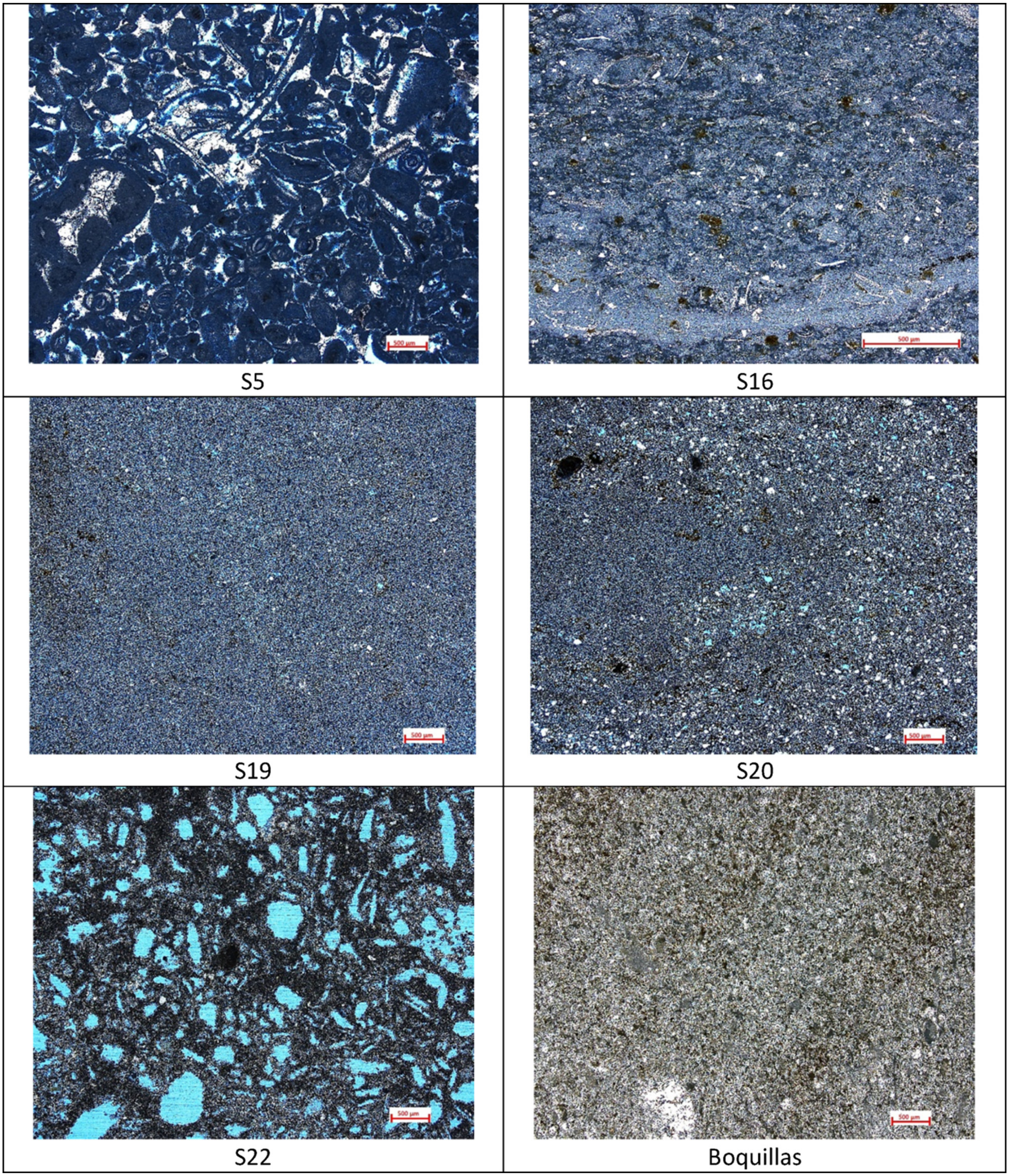

Figure 2 (continued from previous page). Thin-section photomicrographs of all samples. Blue color highlights pore space. Scale bar is 1000 µm for quarried rocks and 500 µm for outcrop samples.

Figure 3. Cross plots of MRH–UCS versus sample volume for the Separate method (top) and the Combined method (bottom) for all studied rock types. Plotting all data on the same scale highlights variation in sample response for each method.

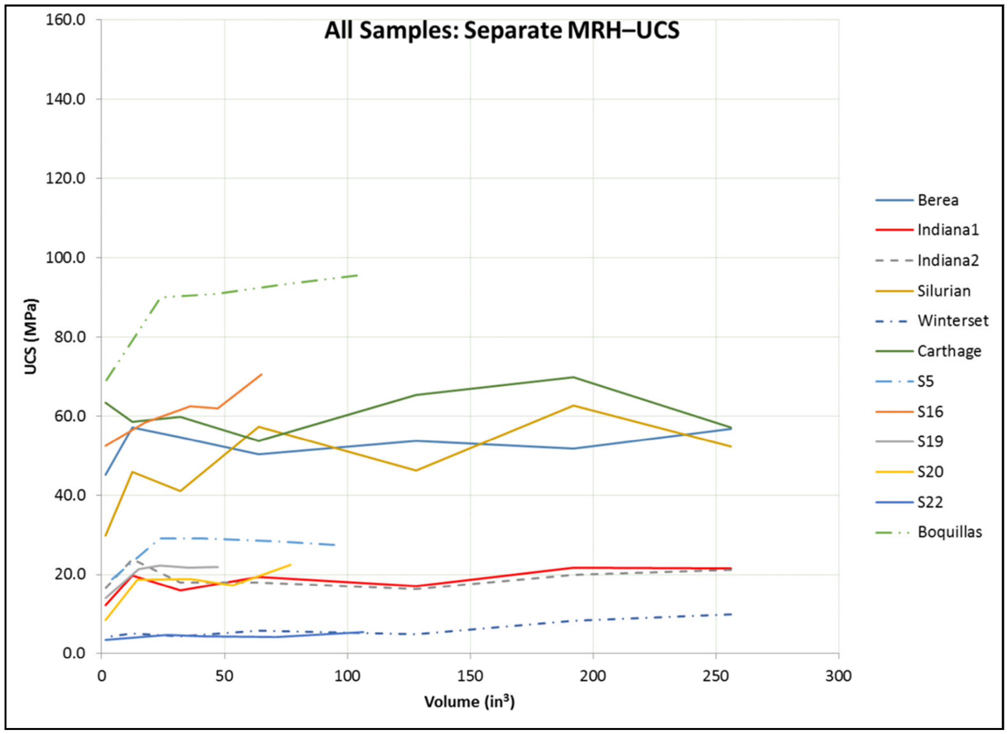

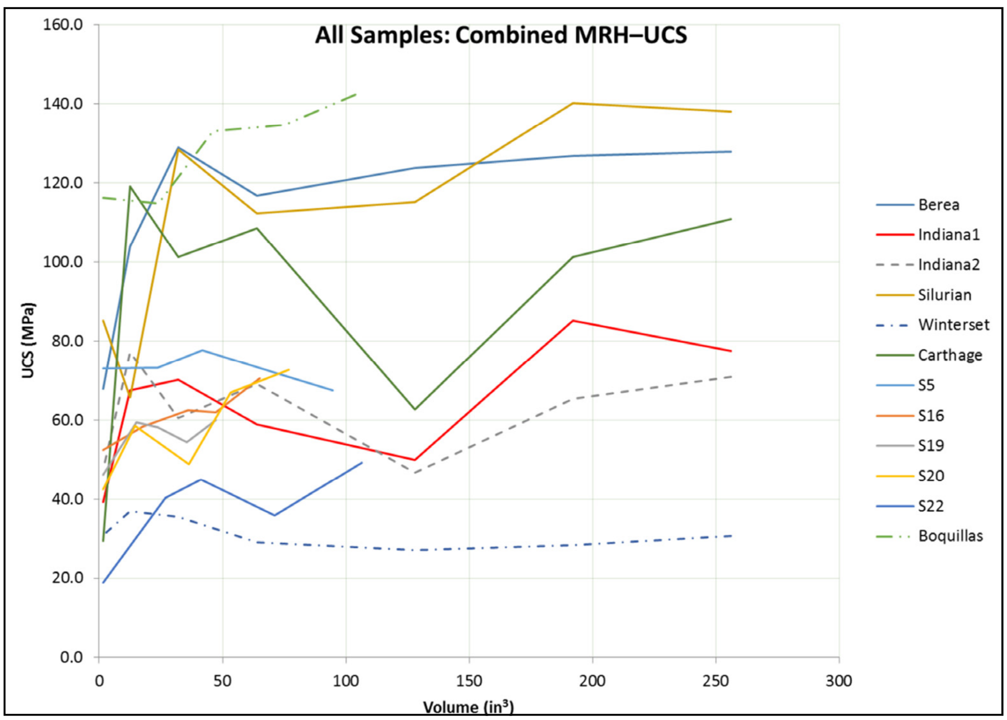

Figure 4 (see **p. 195–197****). Cross plots of MRH–UCS versus sample volume for each rock type measured with the separate method (left) and the combined method (right). The UCS scale varies, depending on the method and rock type, which highlights the difference in data scatter between the two methods. The solid horizontal line indicates average UCS value for samples larger than a 1 in (2.5 cm) plug (2 in^3 [33 cm^3]). Error bars are derived from standard deviations of MRH measurements and propagated through the equation of Zahm and Enderlin (2010).**

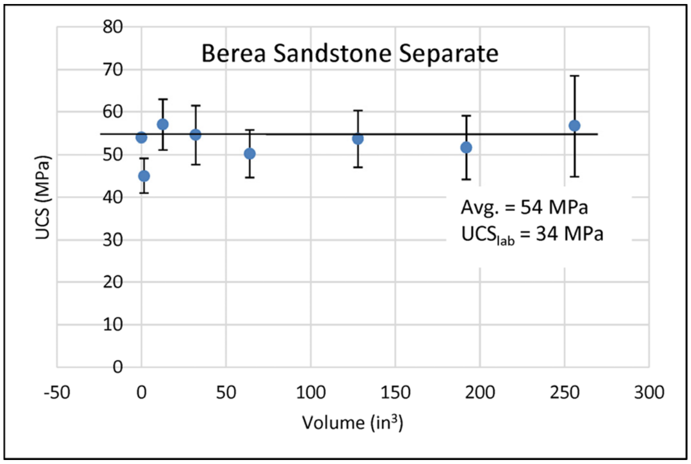
Berea Sandstone Separate
Avg. = 54 MPa
UCS$_{lab}$ = 34 MPa
UCS (MPa)
Volume (in^3)

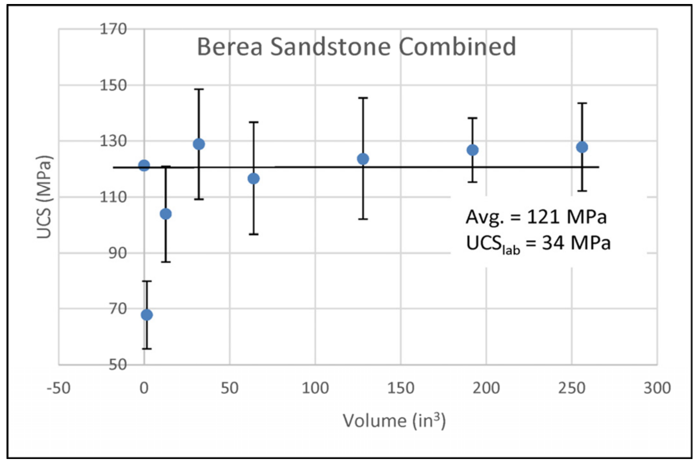
Berea Sandstone Combined
Avg. = 121 MPa
UCS$_{lab}$ = 34 MPa
UCS (MPa)
Volume (in^3)

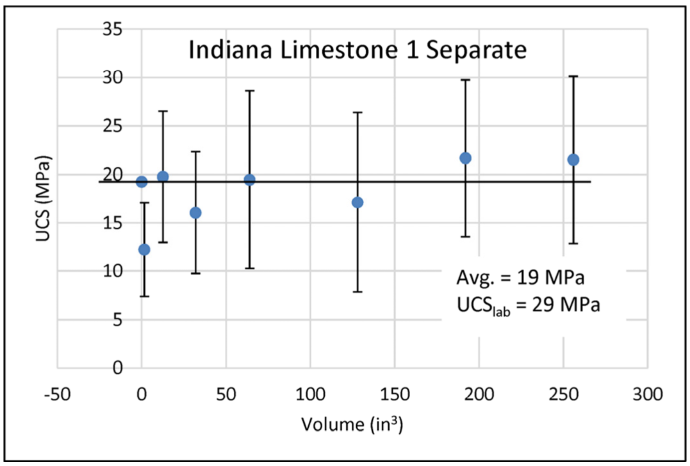
Indiana Limestone 1 Separate
Avg. = 19 MPa
UCS$_{lab}$ = 29 MPa
UCS (MPa)
Volume (in^3)

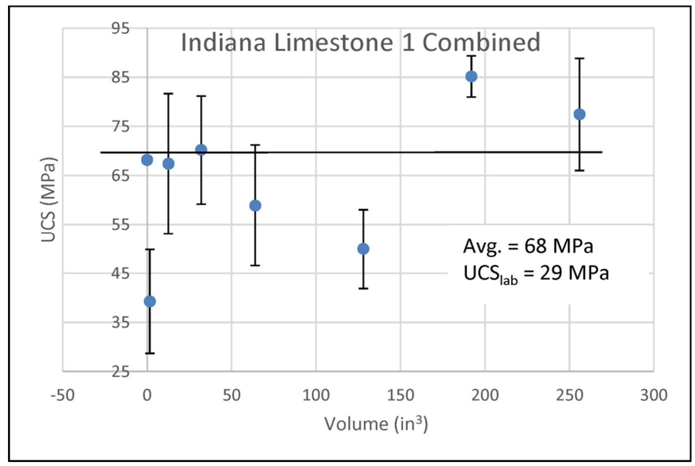
Indiana Limestone 1 Combined
Avg. = 68 MPa
UCS$_{lab}$ = 29 MPa
UCS (MPa)
Volume (in^3)

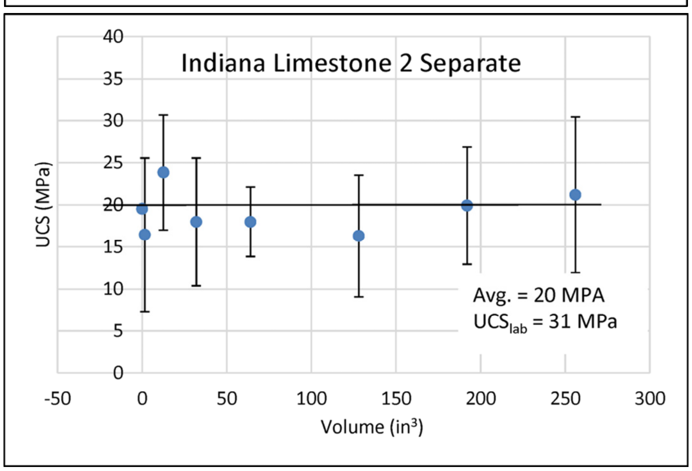
Indiana Limestone 2 Separate
Avg. = 20 MPA
UCS$_{lab}$ = 31 MPa
UCS (MPa)
Volume (in^3)

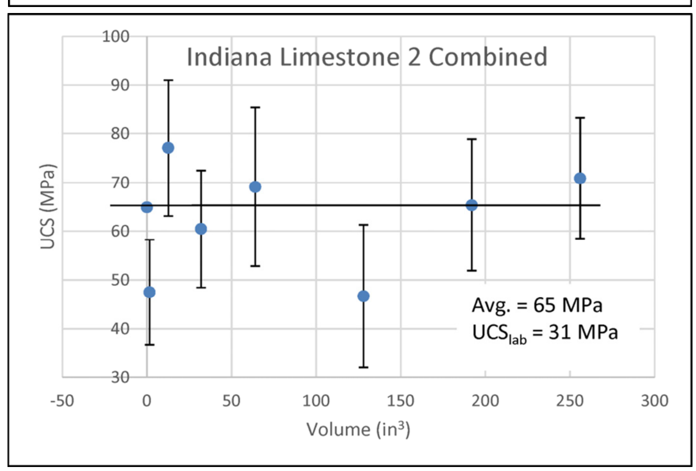
Indiana Limestone 2 Combined
Avg. = 65 MPa
UCS$_{lab}$ = 31 MPa
UCS (MPa)
Volume (in^3)

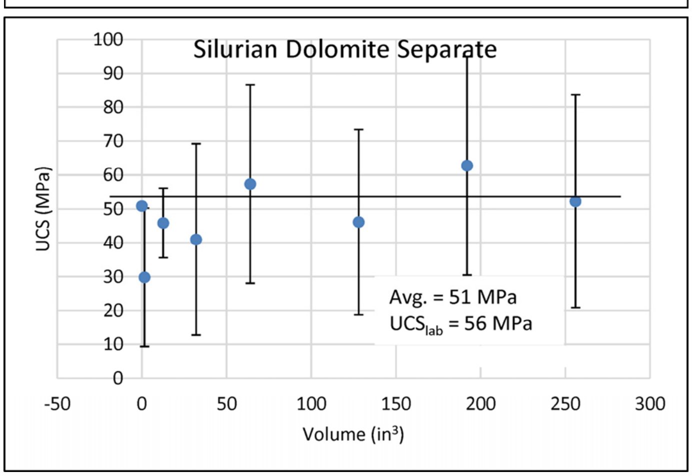
Silurian Dolomite Separate
Avg. = 51 MPa
UCS$_{lab}$ = 56 MPa
UCS (MPa)
Volume (in^3)

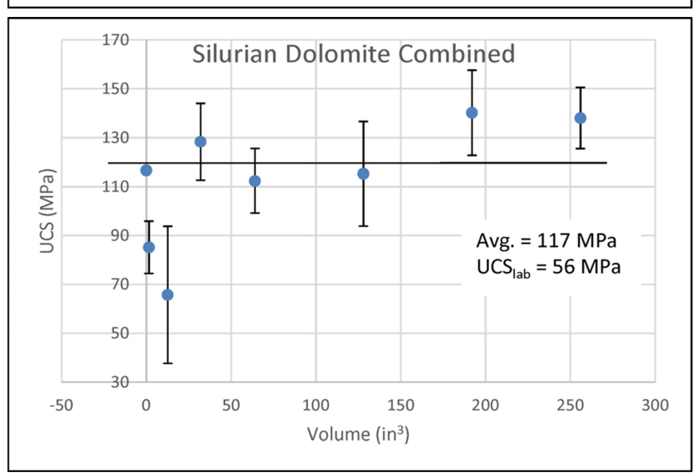
Silurian Dolomite Combined
Avg. = 117 MPa
UCS$_{lab}$ = 56 MPa
UCS (MPa)
Volume (in^3)

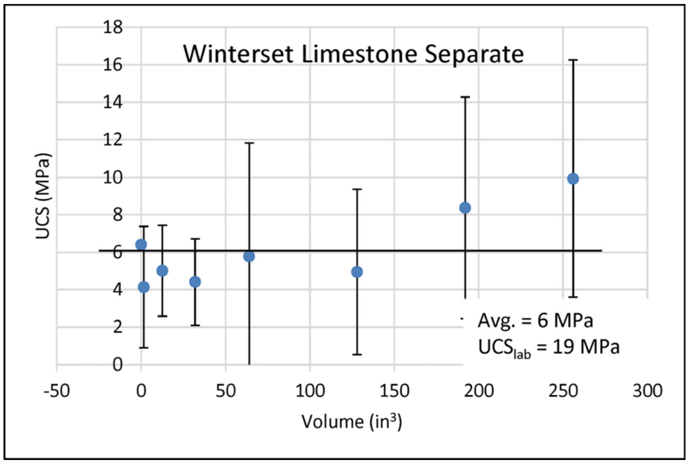
Winterset Limestone Separate
UCS (MPa)
Volume (in³)
Avg. = 6 MPa
UCSlab = 19 MPa

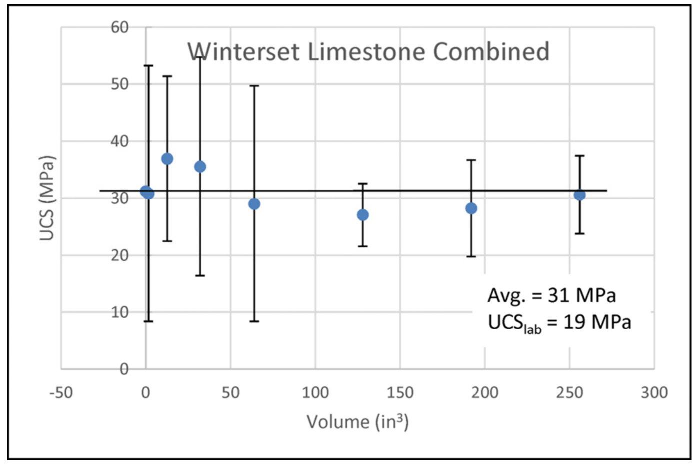
Winterset Limestone Combined
UCS (MPa)
Volume (in³)
Avg. = 31 MPa
UCSlab = 19 MPa

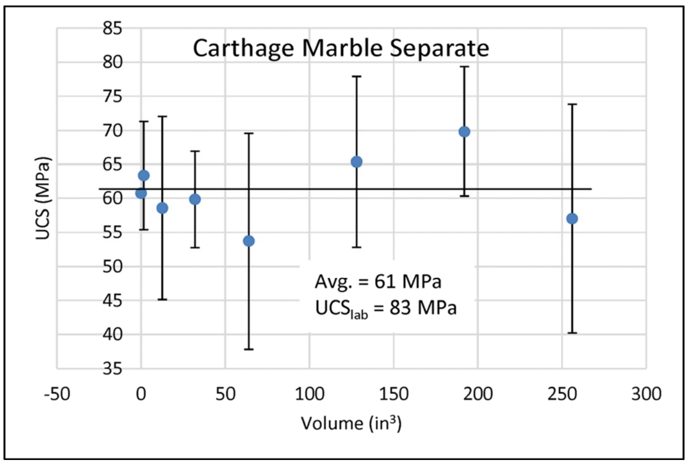
Carthage Marble Separate
UCS (MPa)
Volume (in³)
Avg. = 61 MPa
UCSlab = 83 MPa

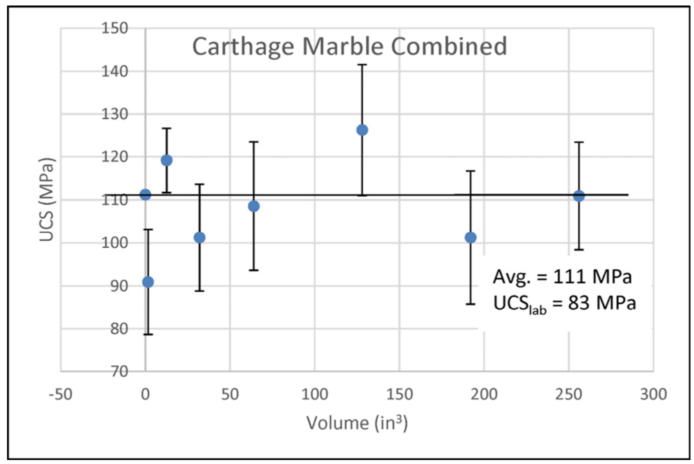
Carthage Marble Combined
UCS (MPa)
Volume (in³)
Avg. = 111 MPa
UCSlab = 83 MPa

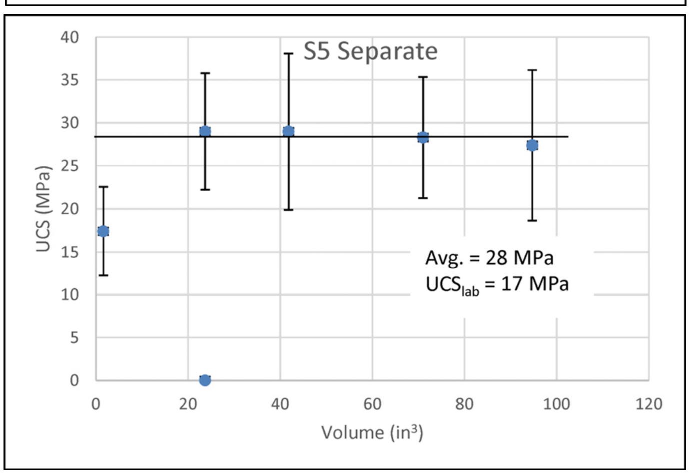
S5 Separate
UCS (MPa)
Volume (in³)
Avg. = 28 MPa
UCSlab = 17 MPa

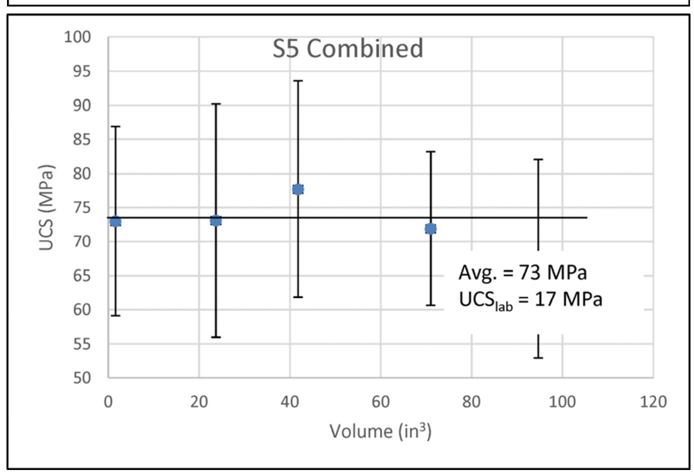
S5 Combined
UCS (MPa)
Volume (in³)
Avg. = 73 MPa
UCSlab = 17 MPa

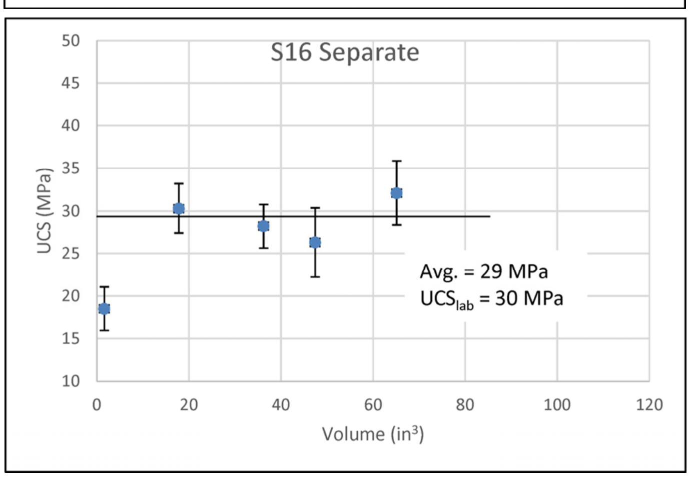
S16 Separate
UCS (MPa)
Volume (in³)
Avg. = 29 MPa
UCSlab = 30 MPa

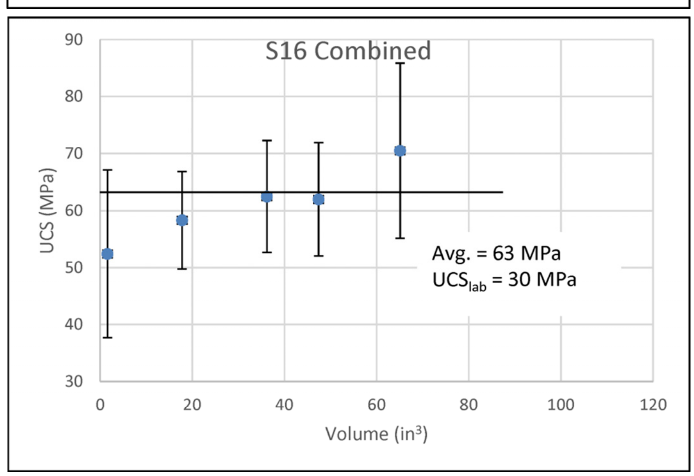
S16 Combined
UCS (MPa)
Volume (in³)
Avg. = 63 MPa
UCSlab = 30 MPa

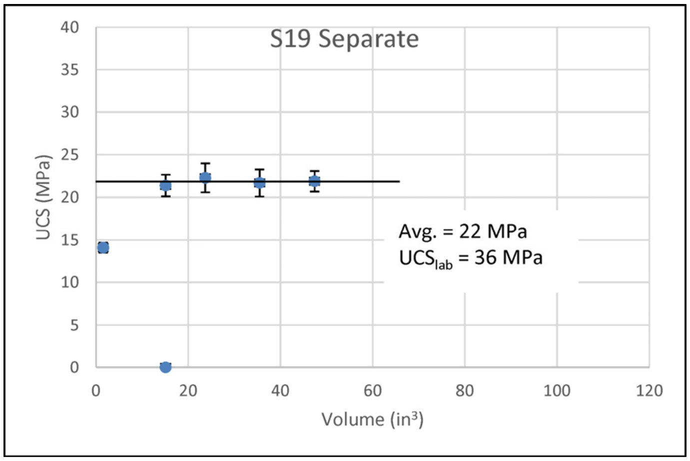
S19 Separate
UCS (MPa)
0 5 10 15 20 25 30 35 40
0 20 40 60 80 100 120
Volume (in³)
Avg. = 22 MPa
UCS$_{lab}$ = 36 MPa

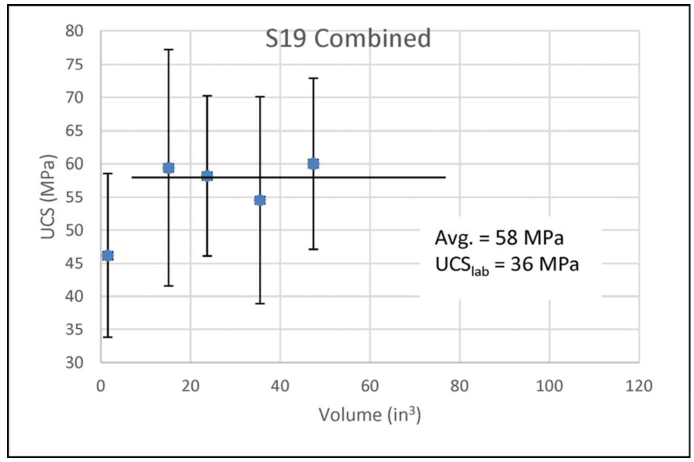
S19 Combined
UCS (MPa)
30 35 40 45 50 55 60 65 70 75 80
0 20 40 60 80 100 120
Volume (in³)
Avg. = 58 MPa
UCS$_{lab}$ = 36 MPa

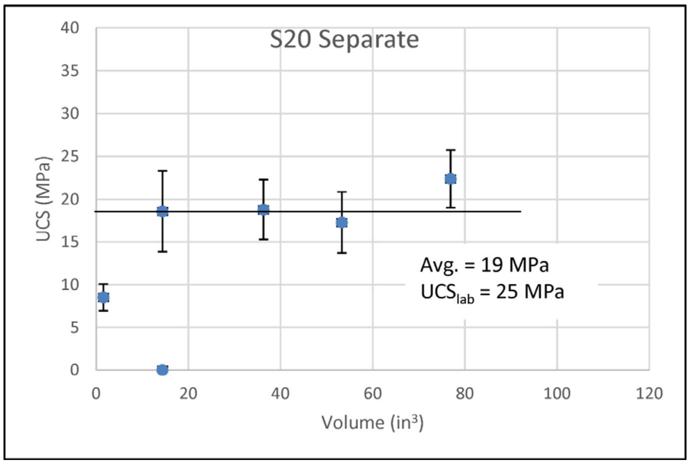
S20 Separate
UCS (MPa)
0 5 10 15 20 25 30 35 40
0 20 40 60 80 100 120
Volume (in³)
Avg. = 19 MPa
UCS$_{lab}$ = 25 MPa

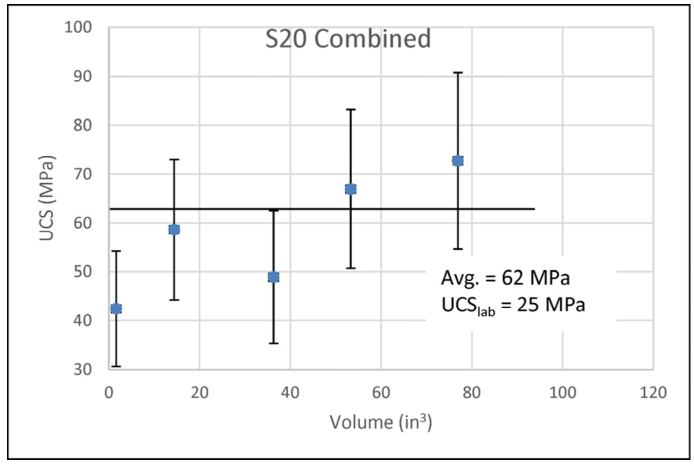
S20 Combined
UCS (MPa)
30 40 50 60 70 80 90 100
0 20 40 60 80 100 120
Volume (in³)
Avg. = 62 MPa
UCS$_{lab}$ = 25 MPa

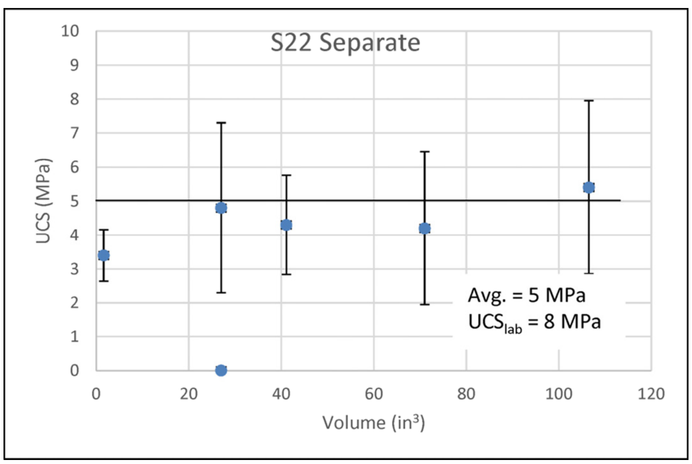
S22 Separate
UCS (MPa)
0 1 2 3 4 5 6 7 8 9 10
0 20 40 60 80 100 120
Volume (in³)
Avg. = 5 MPa
UCS$_{lab}$ = 8 MPa

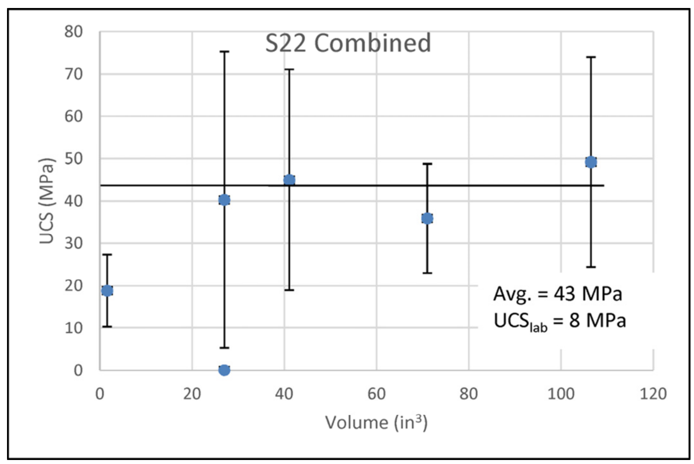
S22 Combined
UCS (MPa)
0 10 20 30 40 50 60 70 80
0 20 40 60 80 100 120
Volume (in³)
Avg. = 43 MPa
UCS$_{lab}$ = 8 MPa

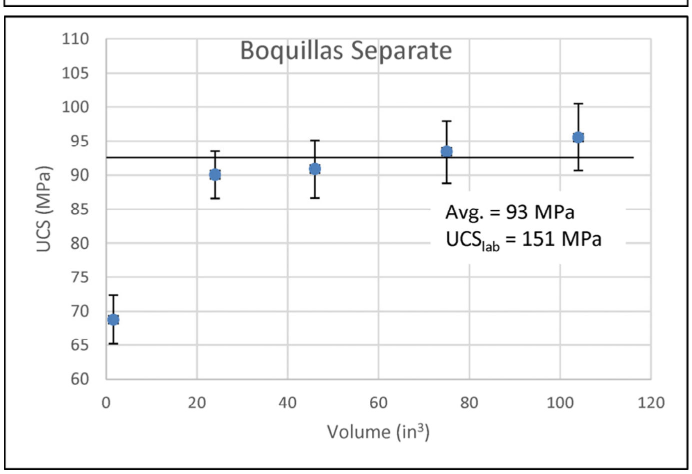
Boquillas Separate
UCS (MPa)
60 65 70 75 80 85 90 95 100 105 110
0 20 40 60 80 100 120
Volume (in³)
Avg. = 93 MPa
UCS$_{lab}$ = 151 MPa

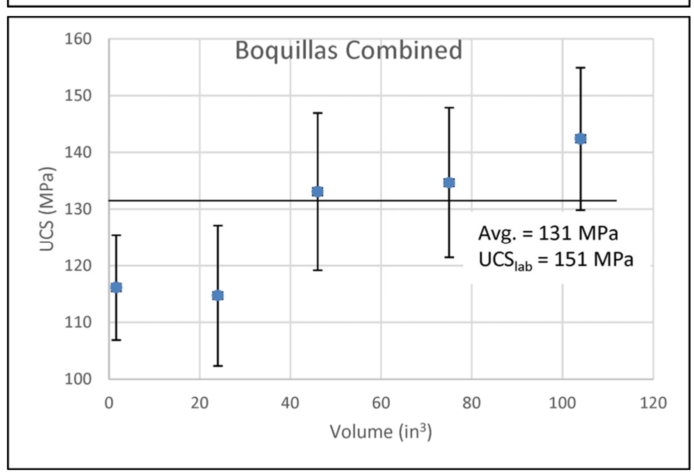
Boquillas Combined
UCS (MPa)
100 110 120 130 140 150 160
0 20 40 60 80 100 120
Volume (in³)
Avg. = 131 MPa
UCS$_{lab}$ = 151 MPa

Table 2. The percent difference between the laboratory UCS measurements for the 1 in plug (UCS_{plug}) and the average of the MRH–UCS measurements for the samples larger than the 1 in plug (UCS_{avg}), for both MRH methods.

Sample		Separate			Combined	
	UCS_{plug}	UCS_{avg}	%Diff	UCS_{plug}	UCS_{avg}	%Diff
Berea Sandstone	45	54	78	68	121	44
Indiana Limestone 1	12	19	16	39	68	43
Indiana Limestone 2	16	20	50	48	65	26
Silurian Dolomite	30	51	92	85	117	27
Winterset Limestone	4	6	950	31	31	0
Carthage Marble	63	61	72	91	111	18
S5	17	28	32	73	73	0
S16	19	29	52	52	63	17
S19	14	22	59	46	58	21
S20	9	19	84	42	62	32
S22	3	5	1280	19	43	56
Boquillas Limestone	69	93	100	116	131	11

Table 3. The percent difference between the laboratory UCS measurements for the 1 in plug (UCS_{plug}) and the MRH–UCS values for the 1 in plug (UCS Sep and UCS Comb) for both MRH methods.

Sample	UCS (lab)	UCS Sep	UCS Comb	Sep %Diff	Comb % Diff
Berea Sandstone	33.9	45.1	67.7	32.9	99.8
Indiana Limestone 1	29.4	12.2	39.3	58.3	33.8
Indiana Limestone 2	30.9	16.4	47.5	46.8	53.7
Silurian Dolomite	55.8	29.8	85.2	46.6	52.6
Winterset Limestone	19.3	4.1	30.8	78.6	59.8
Carthage Marble	83.5	63.4	90.9	22.4	8.9
S5	17	17.4	73	2.4	329.4
S16	30	18.5	52.4	38.3	74.7
S19	36	14.1	46.2	60.8	28.3
S20	25	8.5	42.4	66	69.6
S22	8	3.4	18.8	57.5	135
Boquillas Limestone	151	68.8	116.2	54.4	23

laboratory-derived UCS. Figure 5A shows that the Separate method yielded the better estimation of laboratory-measured UCS compared to the Combined method, which consistently overestimates the UCS. Results for the 1 in (2.5 cm) plugs show that the Combined method is slightly closer to the 1:1 line, mostly because the result for smaller volumes leads to reduced MRH–derived UCS. There, the small volume effect combined with the consistent overestimation of the Combined method gives an artificial result that seems a better approximation. However, we think it would be risky to rely on the combination of two negative effects that produce a good experimental approximation without a solid calibration for each individual dataset.

DISCUSSION

Volume Effect

Verwaal and Mulder (1993) found that the Equotip reported lower results for 1.18 in (30 mm) length cores than for 2.36 in (60 mm) and 3.94 in (100 mm) length cores with the same diameter. Similarly, they found that 1.18 in (30 mm) diameter cores yielded lower results than 1.97 in (50 mm) and 3.94 in (100 mm) diameter cores with the same length. Lee et al. (2014) found that Equotip hardness values for aluminum cylinders declined below 9 in^3 (147 cm^3), possibly due to the proximity of the impact point to a free surface, allowing dissipation of some of the impact energy out of the sample. This study provides similar results. Based on the sample that shows the most consistent behavior, it is clear that the sample-size effect is negligible above 20 in^3 (328 cm^3) and probably also above 12 in^3 (197 cm^3), which is a good approximation of the volume of a standard NX–size plug (2.16 in [5.48 cm] diameter) or NQ–size plug (1.87 in [4.75 cm] diameter) with an ASTM–recommended length-to-diameter ratio of 2.

Influence of Facies, Grain Size, and Cementation on MRH–UCS Data

This study's results show that there is definitive variation between samples, with some having very large scatter of MRH–derived UCS at different volumes and others having very consistent values until reaching a volume threshold, at which point the values begin to decrease sharply. With this current dataset, it is difficult to precisely characterize all the different controls on the MRH–derived UCS on carbonates, but a few patterns emerge.

There is larger scatter in MRH–UCS data for the Silurian dolomites, the Glen Rose bioturbated wackestone (S16), and the bioturbated dolomitic wackestone (S20). These three samples have matrix heterogeneities linked to the bioturbation of the original sediments that were not totally erased by post-depositional diagenesis (Fig. 6). Large scatter is also observed in the Winterset Limestone, which has numerous large (>3/64 in [>1.19 mm]) vuggy pores that are almost impossible to avoid during acquisition (Fig. 6). To a small extent, the Silurian Dolomite also has

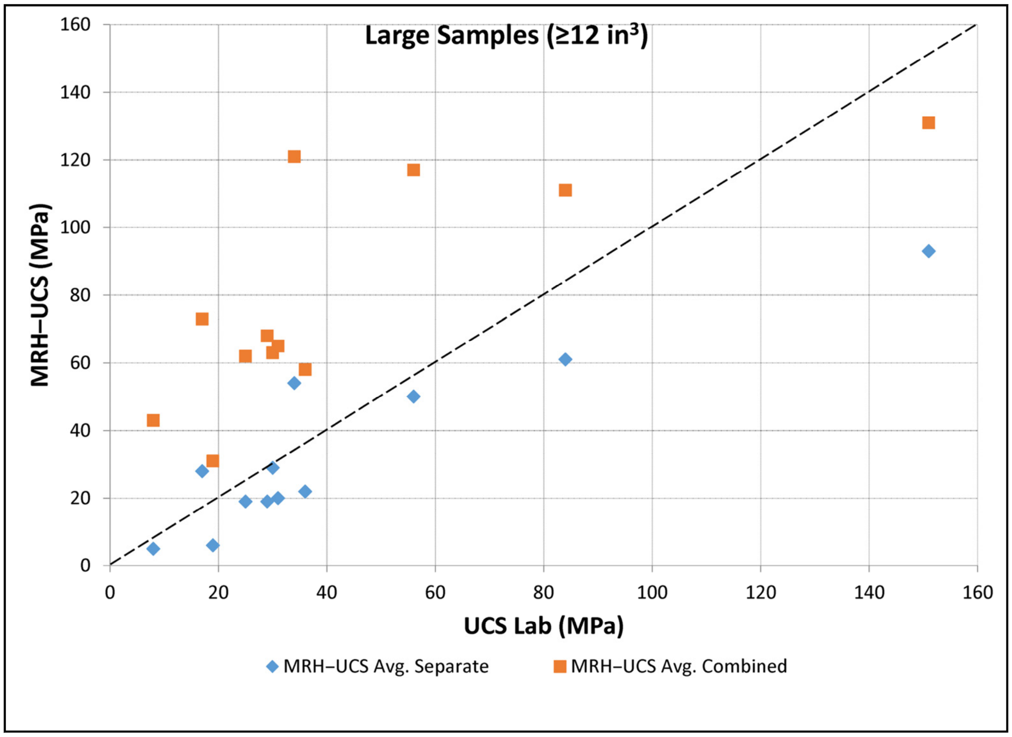

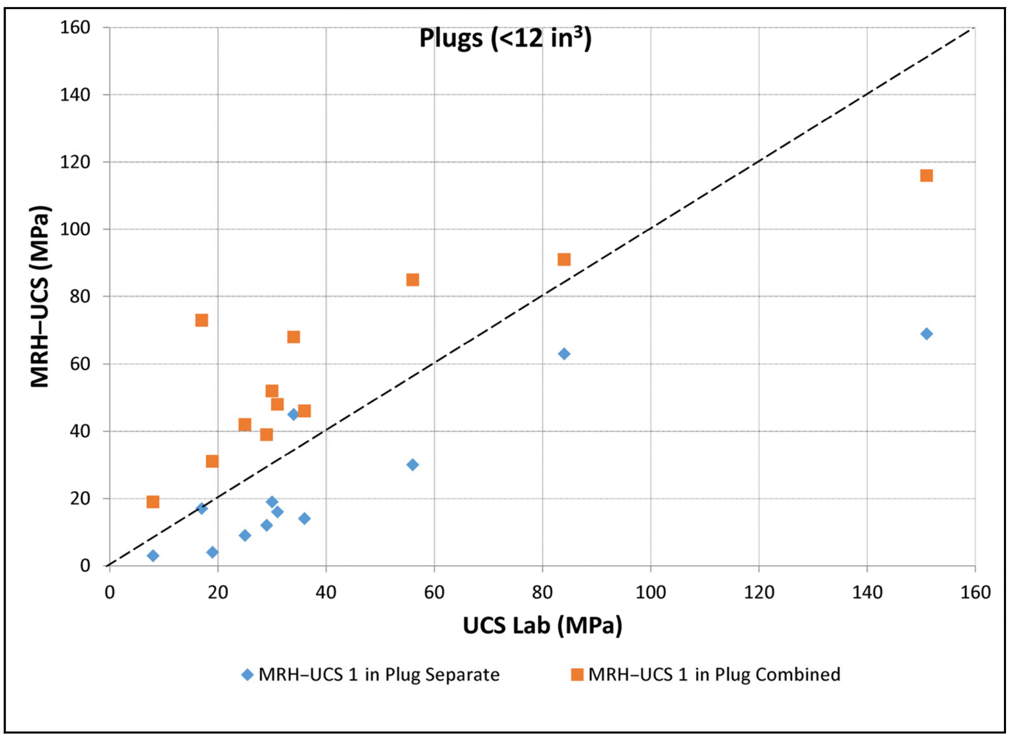

Figure 5. Cross plot of laboratory UCS and MRH–derived UCS: for the average of the large samples (5A), and for the 1 in (2.5 cm) plugs (5B). The dashed line corresponds to the y = x line that would indicate a perfect approximation of laboratory measurement by the MRH method. Orange squares represent measurements made with the Combined method; blue diamonds represent measurements made with the Separate method.

large vuggy pores that should also contribute to the scatter of the MRH–UCS data.

By contrast, the Carthage Marble is a fairly homogeneous rock with rare macropores. The origin of the scatter in the MRH–UCS data for this sample probably originates in the nature of the bioclasts that compose the grainstone (Figs 2 and 6). The large crinoid grains are made of single crystals of calcite. These crinoid grains are actually large enough to be seen macroscopically; it can be speculated that if the MRH tip were pressed on one of those grains, it might yield a higher reading than if the MRH tip lands on the matrix between the grains. The large grain-size effect has been already documented for coarse-grained sandstone by Daniels et al. (2012).

Practical Implications for MRH–UCS Study on Core

This study shows that sample volume starts to influence MRH–device measurements below approximately 12 in^3 (197 cm^3). The results also show that the Separate method leads to the better approximation of the UCS value measured in the laboratory. Whole cores are commonly cut into two parts for preserva-

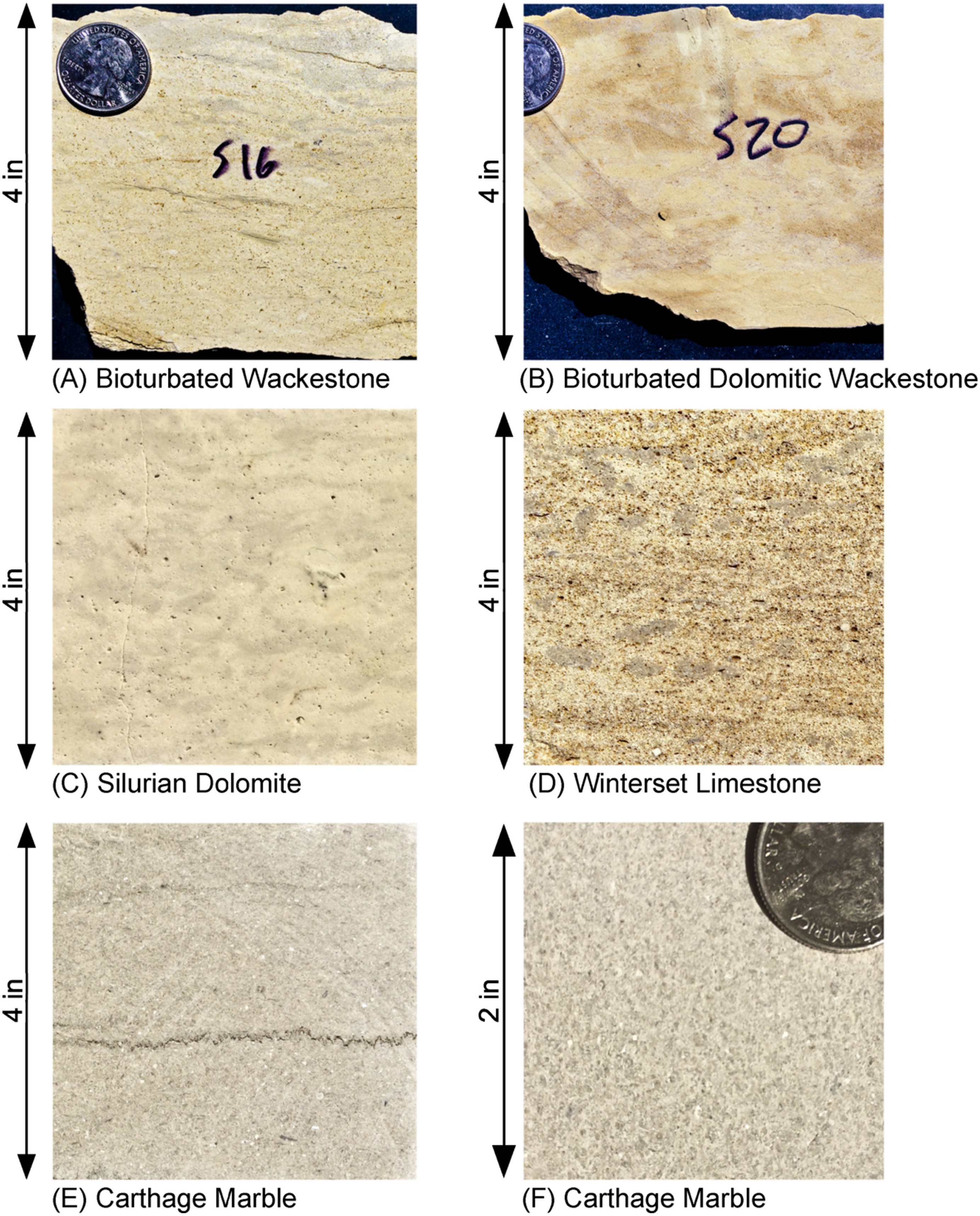

Figure 6. Macroscopic view of samples with heterogeneities. Top shows two Albian bioturbated wackestones. The Silurian Dolomite (middle left) shows the bioturbation in gray. The Winterset Limestone (middle right) shows large moldic pores (dark spots) in the coarse-grained grainstone. Bottom two photos of the Carthage Marble show the large grains that compose the cemented grainstone. Large crinoid grains are visible as either shiny white or gray grains in the enlarged view at the bottom right.

tion in a core depository—a thin part that usually consists of ~1/3 of the core that is used for archiving and geological display. A thicker part, commonly the remaining 2/3 of the core, is used for sample preparation. Our results suggest that MRH–UCS acquisition should preferably be performed on the thick-sample part of the core. Assuming a 3.3 in (8.4 cm) diameter and a 2/3 part of the core, these data suggest that a representative MRH–UCS value with no sample-volume effect would require that MRH measurement be done on a core piece at least 2 in (5 cm) long. If the sample part of a core is not available, performing measurements on the archive part of a core is not necessarily invalid. One should, however, just be aware that the smaller volume will lead to lower MRH–UCS values. Lee et al. (2014) and Ritz et al. (2014) found that MRH–UCS measured on the 2/3 core section tracked more closely with UCS measured in the laboratory than did the same measurements on the 1/3 core section. Lee et al. (2014) also showed that the shape and trend of the two MRH–UCS curves are almost identical and capture reasonably well the UCS trend from laboratory measurement.

An in-house core database of carbonate rocks also shows that MRH–UCS tests on core produce very reasonable results. Figure 7 shows an example of MRH–UCS core data acquired on an Albian core from an oil field along the Stuart City margin in East Texas. MRH–UCS data are plotted alongside acoustic velocity data (captured with a handheld device at the same scale), standard wireline logs, and facies description. This dataset shows that the two independently acquired nondestructive datasets (MRH–UCS and handheld velocity) agreed very well and also matched the density and sonic wireline-log shape remarkably well. Therefore, the relative change in mechanical character is well captured by the MRH method; however, because this dataset was acquired on a thin archive part of the core, the MRH–UCS value should be expected to be smaller than the UCS value measured in the laboratory.

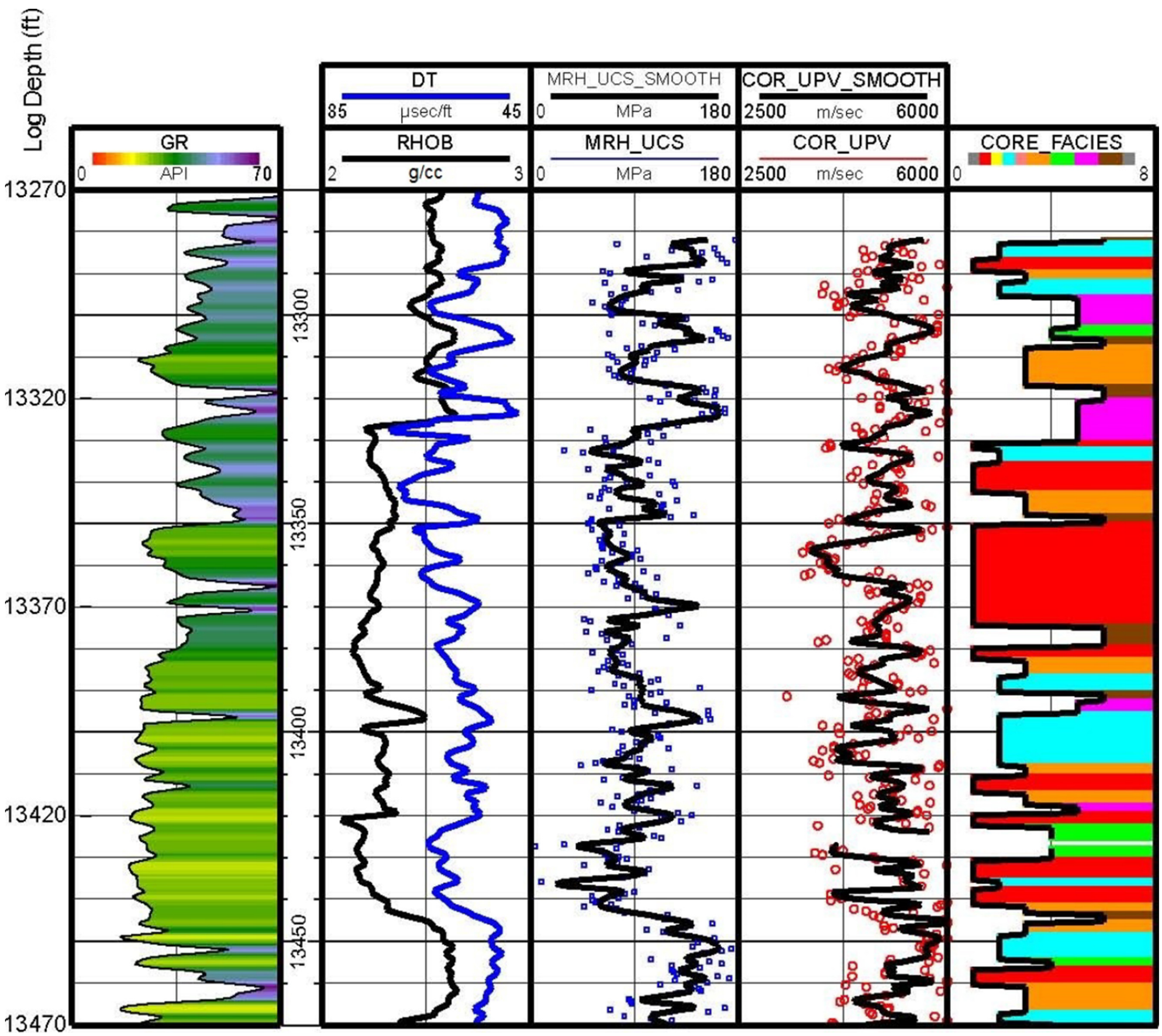

Figure 7. Example of MRH–UCS data for a 200 ft (60 m) core interval of Albian carbonate rocks from a field in East Texas. MRH–UCS data for that core is shown with blue squares in the middle column. The black curve superimposed on the data was made using a 5 sample moving average. The "COR_UPV" data and curve were obtained using a handheld device that measures P–wave velocity. Core description is on right and wireline logs (gamma ray, density, and sonic) are on left.

CONCLUSIONS

Based on the results shown in this paper and the available extensive MRH–UCS database on core, Lee et al. (2014) and Daniels et al. (2012) studies are confirmed and that MRH–UCS data provide a valid approximation for laboratory-measured UCS. The MRH–UCS methods allow for very high resolution stratigraphic acquisition.

Smaller sample volumes yield significant underestimation of the UCS compared to UCS values measured in the laboratory. Scatter in MRH–UCS data is expected when rocks are heterogeneous (bioturbation, laminations), have large macropores, and have large grains. In those cases, careful data acquisition should resolve most of the scattering; however, some of it is intrinsic to the method and to the nature of rock material.

This study found that using the Separate method for acquisition leads to more consistent results, although operators should be aware of the volume effect on MRH–UCS values and the nature of data scatter before using MRH–UCS values for engineering calculations. However, based on the results of this study and an extensive database, the shape and trend of MRH–UCS values acquired on the archive half of cores are very consistent with other high-resolution, nondestructive techniques and wireline log trends and provide valuable data for mechanical characterization of carbonate rocks.

ACKNOWLEDGMENTS

Funding for this study came from the Reservoir Characterization Research Laboratory (RCRL), the State of Texas Advanced Resource Recovery program (STARR), and the industrial sponsors of the Mudrock Systems Research Laboratory (MSRL) at the Bureau of Economic Geology at the University of Texas at Austin. Benjamin Cutright is acknowledged for collecting the non-destructive measurement on the Cretaceous core. This publication was authorized by the Director, Bureau of Economic Geology.

REFERENCES CITED

Aoki, H., and Y. Matsukura, 2008, Estimating the unconfined compressive strength of intact rocks from Equotip hardness: Bulletin of Engineering Geology and the Environment, v. 67, p. 23–29.

Asef, M. R., 1995, Equotip as an index list for rock strength properties: M.Sc. Thesis, International Institute for Geo-Information Science and Earth Observation (ITC), Delft, The Netherlands, 172 p.

Daniels, G., C. McPhee, P. McCurdy, and Y. Sorrentino, 2012, Non-destructive strength index testing applications for sand failure evaluation. Society of Petroleum Engineers Paper SPE–158326–MS, Richardson, Texas, 12 p.

Lee, J. S., L. Smallwood, and E. Morgan, 2014, New application of rebound hardness numbers to generate logging of unconfined compressive strength in laminated shale formations: Proceedings of the 48th U.S. Rock Mechanics/Geomechanics Symposium Paper 14–6972, Minneapolis, Minnesota, 1–4 June, 7 p.

Phelps, R. M., C. Kerans, R. G. Loucks, R. Gama, J. Jeremiah, and D. Hull, 2013, Oceanographic and eustatic control of carbonate platform evolution and sequence stratigraphy on the Cretaceous (Valanginian-Campanian) passive margin, northern Gulf of Mexico: Sedimentology, v. 61, no. 2, p. 1–36.

Ritz, E., M. M. Honarpour, J. Dvorkin, and W. F. Dula, 2014, Core hardness testing and data integration for unconventionals: Society of Petroleum Engineers Paper SPE–2014–1916004–MS, Richardson, Texas, 12 p.

Verwaal, W., and A. Mulder, 1993, Estimating rock strength with the Equotip hardness tester: International Journal of Rock Mechanics, Mining Science and Geomechanics Abstracts, v. 30, p. 659–662.

Viles, H., A. Goudie, S. Grab, and J. Lalley, 2010, The use of the Schmidt hammer and Equotip for rock hardness assessment in geomorphology and heritage science: A comparative analysis: Earth Surface Processes and Landforms, v. 36, p. 320–333.

Zahm, C. K., and M. Enderlin, 2010, Characterization of rock strength in Cretaceous strata along the Stuart City Trend, Texas: Gulf Coast Association of Geological Societies Transactions, v. 60, p. 693–702.